

Cite this: *J. Mater. Chem. A*, 2020, 8, 15900

Do polymer ligands block the catalysis of metal nanoparticles? Unexpected importance of binding motifs in improving catalytic activity†

Lei Zhang,^a Zichao Wei,^a Michael Meng,^a Gael Ung^a and Jie He^{*ab}

Metal nanoparticles (NPs) tethered by synthetic polymers are of broad interest for self-assembly, nanomedicine and catalysis. The binding motifs in polymer ligands usually as the end functional groups of polymers are mostly limited to thiolates. Since the binding motif only represents a tiny fraction of many repeating units in polymers, its importance is often ignored. We herein report the uniqueness of polymeric N-heterocyclic carbene (NHC) ligands in providing oxidative stability and promoting the catalytic activity of noble metal NPs. Two “grafting to” methods were developed for polymer NHCs for pre-synthesized metal NPs in various solvents and with different sizes. Remarkably, imidazolium-terminated polystyrene can modify gold NPs (AuNPs) within 2 min while reaching a similar grafting density to polystyrene-thiol (SH) requiring 6 h modification. We demonstrate that polymer NHCs are extremely stable at high temperature in air. Interestingly, the binding motifs of polymer ligands dominate the catalytic activity of metal NPs. Polymer NHC modified metal NPs showed improved activity regardless of the surface crowdedness. In the case of AuNPs, AuNPs modified with polystyrene NHCs are approximately 5.2 times more active than citrate-capped ones and 22 times more active than those modified with polystyrene thiolates. In view of ligand-controlled catalytic properties of metal NPs, our results illustrate the importance of binding motifs that has been overlooked in the past.

Received 10th April 2020

Accepted 12th May 2020

DOI: 10.1039/d0ta03906c

rsc.li/materials-a

Introduction

Colloidal noble metal nanoparticles (NPs) are of broad interest in heterogeneous catalysis because of their high activity compared to bulk counterparts.¹ Since colloidal NPs are thermodynamically unstable in the absence of capping ligands in solution, there has been tremendous interest in “lighting” with surface ligands of colloidal metal NPs in catalytic cycles.² Surface ligands usually have a strong interaction with the surface atoms of NPs to stabilize colloidal metal NPs from aggregation. However, the passive layer of ligands limits the surface accessibility of NPs, resulting in a major activity loss as reported previously.^{3,4} There are a large number of studies on long alkyl-chain fatty acids/alcohols,^{5,6} amines^{7,8} and thiols⁹ capped on metal NPs that significantly slow down the electron transfer kinetics and therefore block the redox catalysis on the surface of NPs. The surface blocking effect of ligands becomes

worse when using synthetic polymers as ligands since polymers are significantly larger in size compared to small molecule ligands.^{10–14} As inspired by metalloenzymes, the marriage of polymers and noble metal NPs could be used to mimic natural protein frameworks. There are recent examples of polymer/NP hybrid catalysts providing alternative paradigms on the role of polymeric ligands in nanocatalysis, e.g., control of the substrate binding with metal NPs,¹⁵ fine-tuning of the selectivity,¹⁶ and stabilization of reaction intermediates.¹⁷ We recently demonstrated that polymeric ligands controlled the surface accessibility and blocked unwanted reaction pathways.¹⁵ In the electrochemical reduction of CO₂ in aqueous solution, hydrophobic polymer ligands effectively suppressed the reduction of protons by limiting the diffusion of protons through hydrophobic and electronic effects. Yet, the potential of polymer ligands in tuning the catalytic performance of metal NPs has only received sporadic attention.

Thiol-terminated polymers are most commonly used to modify noble metal NPs in the “grafting to” approach through metal–thiolate bonds.^{18–24} The thiolates tend to bind two or three gold atoms on either bridge sites or three-fold hollow sites.²⁵ The Au–S binding has a long bond length of 2.60 Å and a bond energy of 126 kJ mol^{−1}.^{26,27} The Au–C binding, e.g., in the formation of Au bound with N-heterocyclic carbenes (NHCs), is much less studied as polymeric ligands. For the small molecule NHC case, the Au–C binding is much stronger with a bond

^aDepartment of Chemistry, University of Connecticut, Storrs, Connecticut 06269, USA. E-mail: Jie.he@uconn.edu

^bPolymer Program, Institute of Materials Science, University of Connecticut, Storrs, Connecticut 06269, USA

† Electronic supplementary information (ESI) available: Additional synthetic details and characterization of polymers, surface modification of metal NPs, supporting videos to show the ligand modification of NPs, and more kinetic data on the reduction of 4-nitrophenol using AuNPs and PdNPs. See DOI: 10.1039/d0ta03906c

length of 2.03 \AA and a bond energy close to $158 \pm 10 \text{ kJ mol}^{-1}$,^{26,28} implying better stability of NPs through Au–C bonds. Additionally, there is strong electron transfer from ligands to metal through the σ donation of NHCs that leads to an electron-rich surface.^{29,30} In the current contribution, we address the role of binding motifs in polymer ligands, e.g., metal–S and metal–C binding (Scheme 1), in tuning the activity of noble metal NPs, despite a similar surface crowding effect (Scheme 1). We first developed two “grafting to” methods to modify colloidal noble metal NPs with polymeric NHCs that are far less studied compared to thiol-terminated polymers. We demonstrate that, given the almost identical polymer chains in terms of chemical nature and grafting density, the nature of the binding motif (metal–NHC > metal–S) is key to significantly improve the stability and catalytic activity of NPs. In the case of Au, AuNPs modified with Au–NHC are approximately 6 times more active than citrate-capped ones and 22 times more active than those modified with Au–S using the reduction of 4-nitrophenol as a model reaction. Our ligand exchange methods likely provide a general guideline to modify and stabilize noble metal NPs with NHCs, while promoting their catalytic activity simultaneously.

Results and discussion

The surface modification of metal NPs was carried out using end-group functionalized polystyrene (PS) ligands. To generate metal–NHC modification, two different PS ligands were prepared, namely methylimidazolium bicarbonate terminated PS (PS₄₀–Im HCO₃[–], $M_{n,SEC} \approx 8.2 \text{ kg mol}^{-1}$ and dispersity \mathcal{D} of 1.07, denoted as P1 hereafter, Fig. S1†) and copper NHC terminated PS (PS₄₀–NHC–Cu, $M_{n,SEC} \approx 8.3 \text{ kg mol}^{-1}$ and \mathcal{D} of 1.08, P2, Fig. S1) (see their syntheses in the ESI†). Using AuNPs as an example, 14 nm citrate capped AuNPs (Au–CA) were prepared first by reducing HAuCl₄ with sodium citrate.³¹ The modification of AuNPs with P1 was performed in pure water where the tetrahydrofuran (THF) solution of P1 (10 mg mL^{–1}) was injected under stirring. Since water is a poor solvent for PS, crashing out of P1 together with AuNPs was seen within 2 min (Fig. 1b and ESI Video 1†). The ligand exchange is so fast that bound AuNPs crashed out together with PS in water since water is a poor solvent for PS. This is unlike the traditional ligand

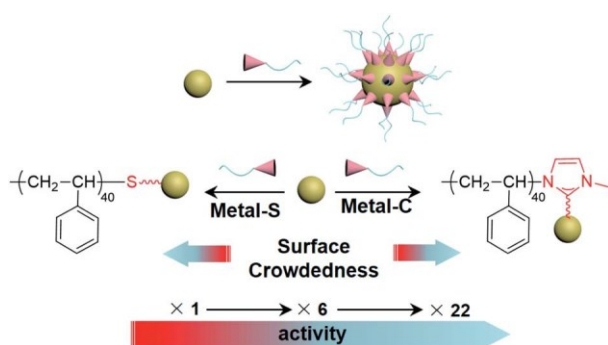
exchange that requires mixing for hours to days. After removal of the aqueous layer, P1-modified AuNPs (or Au–P1) were centrifuged and re-dispersed in THF, and further purified with THF four times (see ESI† for purification details). During purification, unbound polymers and other molecular species that cannot be centrifuged down were removed completely as described previously.³⁴

For P2, the surface modification was performed at the biphasic interface of water and toluene.³² The aqueous solution containing Au–CA was mixed with a toluene solution of P2 (1 mg mL^{–1}). After stirring for 4 min, AuNPs transferred from water to toluene as evidenced by the color change in different layers (Fig. 1f and ESI Video 2†). Again, the phase transfer of AuNPs is so fast that stirring for hours is unnecessary to obtain high grafting density (see below). The purification of Au–P2 is similar to that of Au–P1. The two methods are unique for each polymer and cannot be exchanged. Specifically, P1 with an imidazolium end group is positively charged; and it causes electrostatic aggregation of Au–CA instantly when modifying in a good solvent of P1. Meanwhile, P2 with NHC–Cu is a mild ligand and it modifies AuNPs through either transmetalation or Cu–Au binding.^{32,33} So, P2 cannot modify Au–CA in a poor solvent of PS, likely due to the slower binding to AuNPs.

Thiol-terminated PS (PS₄₀–SH, $M_{n,SEC} \approx 7.9 \text{ kg mol}^{-1}$ and \mathcal{D} of 1.21, P3) was further used as a control to modify AuNPs. The surface modification was carried out in dimethylformamide (DMF), a good solvent of PS, as developed by Nie et al.^{34,35} The binding of thiol-terminated PS to AuNPs is much slower compared to the first two polymers and a minimum of 2 h is required to obtain reasonably stable Au–P3 (Fig. 1j). Alternatively, the surface modification using P3 could be conducted using the biphasic transfer method described for P2, but took a minimum of 12 h to transfer Au–CA from the aqueous phase.

The change of surface ligands can be verified by the solubility of PS-tethered AuNPs. PS-modified AuNPs (Au–P_n, $n = 1–3$) are no longer dispersible in water, while they can be readily dispersed in any good solvents of PS, such as DMF, 1,4-dioxane, anisole, dichloromethane (DCM), THF, toluene, and dimethylacetamide (DMAc) (Fig. 1c, g and k). The localized surface plasmon resonance (LSPR) peak of Au–CA is at $\approx 520 \text{ nm}$ in water. Meanwhile, the LSPR peaks of Au–P1, Au–P2 and Au–P3 were observed at 520–530 nm in organic solvents (Fig. 1d, h and l), indicating that polymer-modified AuNPs were stable in those solvents. There is a slight redshift of the LSPR peak compared to that of Au–CA in water, due to the difference in the refractive index among solvents relative to water and the presence of polymer ligands on the surface of AuNPs.¹⁵ Additionally, nanostructures of Au–P1, Au–P2 and Au–P3 were examined by transmission electron microscopy (TEM) and corresponding size distribution. After modification, there is no apparent change in the average size and shape of AuNPs modified by all three polymers (Fig. S2†).

We used proton nuclear magnetic resonance (¹H NMR) and 2D heteronuclear multiple bond correlation (HMBC) spectroscopy to confirm successful modifications of AuNPs with two PS–NHCs. Both Au–P1 and Au–P2 show characteristic resonance peaks of PS, including the aromatic protons around 7 ppm and



Scheme 1 Surface ligand modification of noble metal NPs.

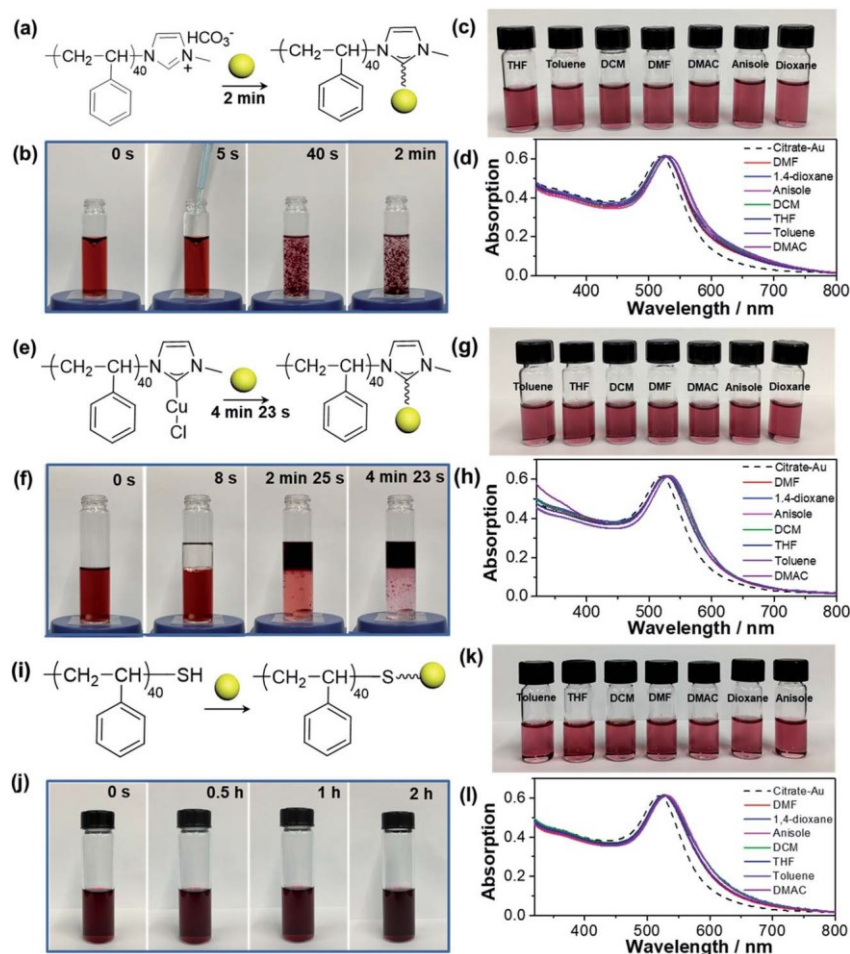


Fig. 1 Surface modification of AuNPs using (a–d) P1, (e–h) P2 and (i–l) P3. (b), (f) and (j) show the corresponding images during surface modification. The images and UV-vis spectra of (c and d) Au–P1, (g and h) Au–P2 and (k and l) Au–P3 were dispersed in various good solvents of PS.

the protons from the PS backbone at 1–2 ppm (Fig. S3a and b†). As previously observed in small molecule NHC ligands, the imidazolium salt with bicarbonate counter ions is known to convert the NHC quickly at r.t. or heating at 40–50 °C.²⁸ This is similar to that of P1 to bind AuNPs. For unbound P1, the N–CH–N of the imidazolium shows a broad peak at 10.4 ppm. The disappearance of this peak for Au–P1 is seen. This is indicative of the formation of Au–C binding upon the removal of N–CH–N as reported previously.¹⁵ For Au–P2, the ¹H NMR and ¹³C NMR spectroscopic features are similar to that of Au–P1 (Fig. S3 and S4†).

HMBC experiments were carried out to identify the presence of NHCs through the coupling of protons with carbon in order to compare the two polymeric NHC modified AuNPs (Fig. 2, S4 and S5†). For all HMBC spectra, the cross peaks of the aromatic carbons (C₆–C₉ in Fig. 2) of PS at 126–128 ppm and the aromatic protons at 6.6–7.1 ppm (H₇–H₉ in Fig. 2) are observed regardless of AuNPs. The peak intensity is much less for Au–P1 and Au–P2, due to the lower concentration of polymer. Other cross peaks from the backbone of PS from carbons at 35–40 ppm (C₅) and protons at 6.6 ppm (H₇) are characteristic of the PS ligands. For

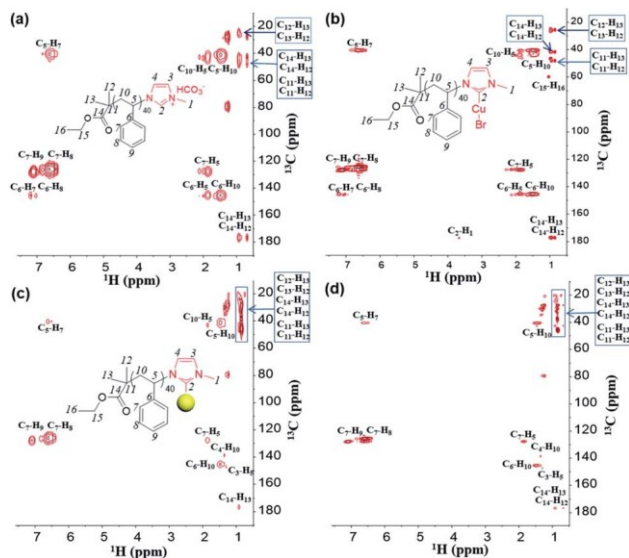


Fig. 2 2D HMBC spectra of (a) P1, (b) P2, (c) Au–P1 and (d) Au–P2. The HMBC spectra were collected in CDCl₃ with 50 mg mL⁻¹ AuNPs.

Au-P1, a set of new peaks appeared in comparison with pure P1. The cross peaks from the carbon at 138.6 ppm assigned to C₄ and the proton at 1.35 ppm assigned to H₁₀ as well as the carbon signal at 147 ppm assigned to C₃ and the proton at 1.3 ppm assigned to H₅ were observed through virtual coupling. This is attributed to cross coupling of vinyl carbons of NHCs and protons in the backbone of PS. All those peaks can be seen in Au-P2 which is indicative of the existence of NHCs as the binding motifs on the surface of Au-P1 and Au-P2.

The grafting density of the three polymers on the AuNPs was evaluated through thermogravimetric analysis (TGA, Fig. S6†). The grafting density of P1 and P2 is 0.35 and 0.29 chains per nm², respectively (Table 1), both of which are comparable to the grafting density of P3 (0.20 chains per nm²) with a similar molecular weight. Such grafting density of three polymers is relatively low and is typical for the “grafting to” approach.³⁶ A similar grafting density also excludes the influence of polymer density on the catalysis of NPs, as discussed below.

We further confirm the versatility of our surface modification methods using different sizes of AuNPs. AuNPs capped with CA in the size range of approximately 3 nm (denoted as “-3 nm”) to “-44 nm”) were synthesized by a seed-mediated growth method (see ESI† for details).³⁷ Along with the size of AuNPs, the LSPR peak of Au displayed a redshift from 505 nm to 535 nm (Fig. S7†). The protocol for the surface modification was similar to that used for “-14 nm AuNPs (Fig. S8 and S9†). It was noteworthy that the solution of “-3 nm Au-P1 only turned turbid without obvious precipitation. This phenomenon is reasonable since the size of “-3 nm Au is too small to bind many polymers and results in co-precipitation in water. Fig. 3a–c displays the UV-vis spectra of AuNPs with different sizes before and after modification with P1 and P2. Regardless of the size of AuNPs, a slight redshift was observed when AuNPs were modified with PS ligands. No new peak appeared at longer wavelengths, suggesting that all modified AuNPs are well soluble in the good solvents of PS. The TEM images and corresponding size distribution of AuNPs with different sizes after modification further confirmed the retained morphology and size of AuNPs (Fig. 4a₁–c₃).

Our ligand exchange approach can be extended to AuNPs with other capping ligands, like oleylamine. For P1, the surface modification of oleylamine capped AuNPs (Au-OAm) was carried out in a good solvent of PS, e.g., DCM. Typically, Au-OAm was first dispersed in DCM and a DCM solution of P1 (10 mg mL⁻¹) was added dropwise. The modification of P2 was exerted in the two phases of hexane and DMF. As shown in Fig. S10,† the original Au-OAm was dispersed in hexane at the top layer. After injecting the DMF solution of P2, the AuNPs can

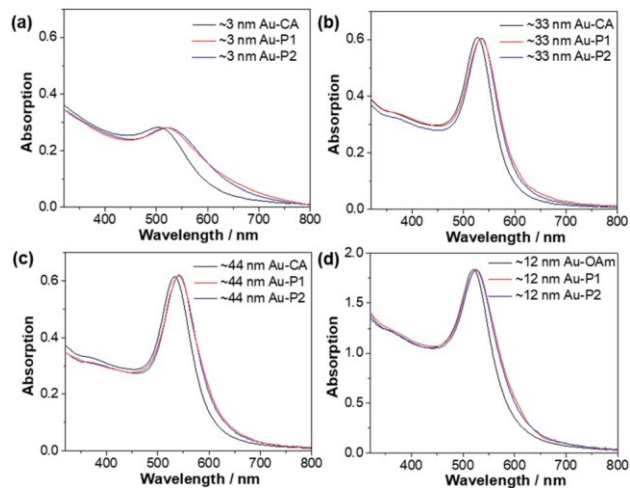


Fig. 3 UV-vis spectra of (a) “-3 nm Au-CA, (b) “-33 nm Au-CA, (c) “-44 nm Au-CA and (d) “-12 nm Au-OAm before and after surface modification with P1 and P2. The solvent for NPs after modification is THF.

be successfully transferred from the hexane layer (top) into the DMF layer (bottom) within 30 min. As characterized by TEM and UV-vis (Fig. 3d and 4d₁–d₃), the grafting of P1 and P2 was confirmed in the OAm-capped NP system. In addition, the ligand exchange of CTAB-capped AuNPs with P1 and P2 was rather difficult possibly due to the electrostatic repulsion between the polymers and positively charged CTAB.

Other noble metal NPs, such as PdNPs and PtNPs, were also investigated. Citrate capped PdNPs (Pd-CA) were prepared by reducing PdCl₂ with sodium citrate.³⁸ And citrate capped PtNPs (Pt-CA) were obtained by using NaBH₄ to reduce K₂PtCl₆.³⁹ Similar to that of AuNPs, the modification of P1 and P2 for PdNPs and PtNPs was conducted in pure water and the biphasic interface, respectively. As shown in Fig. 5a, a THF solution containing P1 (10 mg mL⁻¹) was injected into the aqueous solution of PdNPs. The mixture immediately changed to turbid and as-resultant Pd-P1 was collected by centrifugation. Note that the solution of PdNPs is more dilute compared to that of AuNPs and only a turbid solution, instead of the precipitation seen for AuNPs, was observed. For P2, after placing the toluene solution of P2 on top of the aqueous solution Pd (Fig. 5b), the phase transfer of PdNPs occurred within 1 min. Similarly, Pt-P1 and Pt-P2 were also obtained (Fig. 5c and d). As revealed by TEM images and corresponding size distributions, polymer-modified PdNPs and PtNPs retain their nanostructures and original sizes (Fig. 5). This further implies that our surface

Table 1 Summary of molecular weights and dispersity of the three polymers and their grafting density on AuNPs

Polymers	M _{n,NMR} (kg mol ⁻¹)	M _{n,SEC} (kg mol ⁻¹)	Đ (M _w /M _n)	Grafting density (chains per nm ²)
PS ₄₀ -Im HCO ₃ ⁻ (P1)	4.5	8.3	1.08	0.35
PS ₄₀ -NHC-Cu(i) (P2)	4.5	8.2	1.07	0.29
PS ₄₀ -SH (P3)	4.3	7.9	1.21	0.20

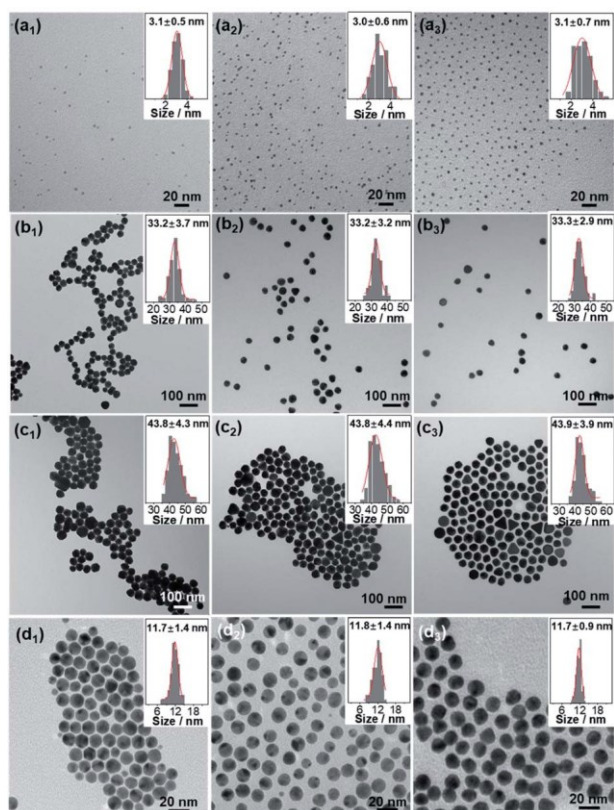


Fig. 4 TEM images and corresponding size distribution of (a₁–a₃) "–3 nm Au–CA, Au–P1, Au–P2, (b₁–b₃) "–33 nm Au–CA, Au–P1, Au–P2, (c₁–c₃) "–44 nm Au–CA, Au–P1, Au–P2 and (d₁–d₃) "–12 nm Au–OAm, Au–P1, Au–P2.

modification method to generate metal–NHC binding for polymer ligands is universal for noble metal NPs.

Metal–thiolate binding has been known to be unstable under oxidative conditions as shown in the early studies of self-assembly monolayers.⁴⁰ The oxidation of thiolate to sulfoxide and sulphone results in the debinding with metals. We have compared the binding stability of Au–NHC with Au–S. The stability of all polymer-modified AuNPs was examined in DMF at 110 °C under air. As monitored by UV-vis spectroscopy, the LSPR peak of Au–P1 and Au–P2 displayed no obvious change. The color of both solutions was red as given in the corresponding pictures before and after thermal treatment (Fig. 6a and b). In contrast, the LSPR peak of Au–P3 showed a clear broadening after 1.5 h heating at 110 °C. The color of the Au–P3 solution changed from red to dark blue after 3 h, suggesting that Au–P3 is not stable at 110 °C in the presence of air (Fig. 6c). This is likely due to the partial removal of P3 from the surface of AuNPs by the –SH group as suggested by previous reports.⁴⁰ Compared with Au–S, the Au–NHC binding is more robust and stable which is of critical importance to study the role of ligands in oxidation reactions. In addition, the stability of PS-modified AuNPs against the competitive small molecule ligand, dithiothreitol (DDT), was also investigated.⁴¹ In the presence of 1.5 M DDT, a slight redshift and peak broadening were found for Au–

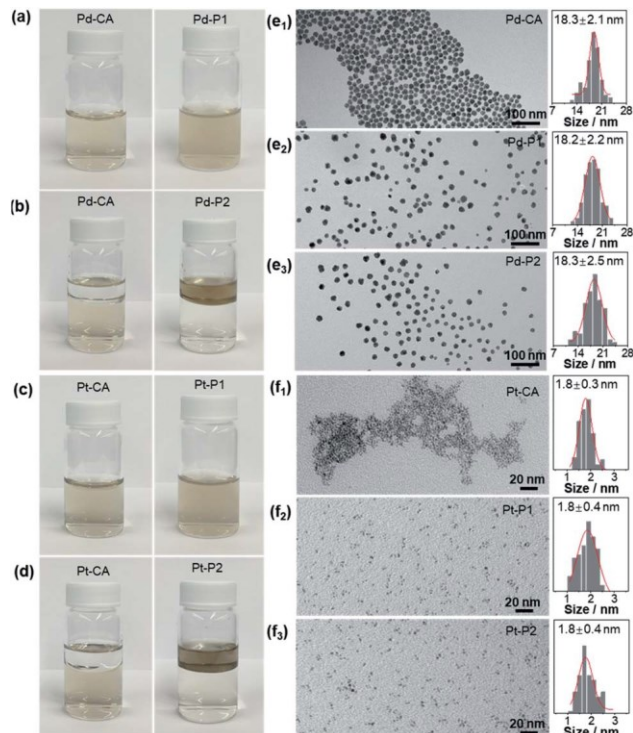


Fig. 5 (a–d) The pictures of (a and b) Pd–CA and (c and d) Pt–CA before and after modifications with P1 and P2. The corresponding TEM images and size distribution of (e₁) Pd–CA, (e₂) Pd–P1, (e₃) Pd–P2, (f₁) Pt–CA, (f₂) Pt–P1, and (f₃) Pt–P2.

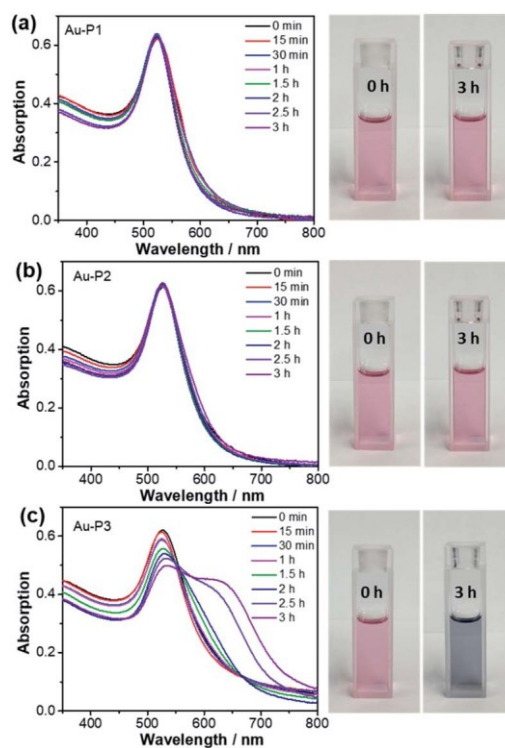


Fig. 6 UV-vis spectra and corresponding digital images of (a) Au–P1, (b) Au–P2 and (c) Au–P3 at 110 °C before and after thermal treatment.

P3 over 1 h (Fig. S11c†), while it showed a minimum impact on Au-P1 and Au-P2 over 1 h (Fig. S11a and b†).

We further evaluated the catalytic activity of polymer-modified AuNPs using the reduction of 4-nitrophenol by NaBH_4 as a model reaction (Fig. S12†).⁴² The reduction kinetics of 4-nitrophenol was monitored by UV-vis using the absorption peak of 4-nitrophenolate at ~ 400 nm (Fig. 7a–d). The reduction of 4-nitrophenol using different catalysts was repeated three times to ensure the reproducibility of catalysis (Fig. S13–S16†). When adding polymer-tethered AuNPs, there is an obvious trend in the decreased rate of the absorbance at ~ 400 nm. The reactions catalyzed by Au-P1 and Au-P2 are significantly faster compared to those with Au-CA and Au-P3. With Au-CA, 9 min was needed to get the full conversion of 4-nitrophenol, while, with Au-P1 and Au-P2, the reduction completed within 130 s. In contrast, Au-P3 showed a poor activity and the full reduction of 4-nitrophenol reached ca. 24 min.

The rate constant (k) of the reduction reaction can be extracted from the relative absorbance change (A/A_0) of 4-nitrophenol at 400 nm against the reaction time (s),⁴³ where A and A_0 respectively represented the absorbance at a given reaction time and the initial state, respectively. The reduction of 4-nitrophenol usually follows the first-order kinetics according to the classic Langmuir–Hinshelwood mechanism.⁴⁴ For reactions with Au-P1, Au-P2 and Au-CA, the reaction kinetics fit well with two reaction rate constants where a fast reaction rate

Table 2 The average rate constant of nitrophenol reduction using different catalysts calculated from three independent tests

Catalysts	Rate constant k (s^{-1})	
Au-P1 ^a	k_1 $\frac{1}{4} -0.04 \pm 0.006$	k_2 $\frac{1}{4} -0.009 \pm 0.003$
Au-P2 ^a	k_1 $\frac{1}{4} -0.028 \pm 0.006$	k_2 $\frac{1}{4} -0.010 \pm 0.002$
Au-P3 ^a	k $\frac{1}{4} -0.0018 \pm 0.0001$	
AuNPs ^a	k_1 $\frac{1}{4} -0.0077 \pm 0.0012$	k_2 $\frac{1}{4} -0.0023 \pm 0.0012$
Pd-P1 ^b	k_1 $\frac{1}{4} -0.014 \pm 0.001$	k_2 $\frac{1}{4} -0.002$
Pd-P2 ^b	k_1 $\frac{1}{4} -0.012 \pm 0.001$	k_2 $\frac{1}{4} -0.002$
Pd-P3 ^b	k $\frac{1}{4} -0.001$	
PdNPs ^b	k_1 $\frac{1}{4} -0.0043 \pm 0.0006$	k_2 $\frac{1}{4} -0.001$

^a The concentration of Au catalysts is 4.9×10^{-3} mg mL^{-1} . ^b The concentration of Pd catalysts is 7×10^{-4} mg mL^{-1} .

(k_1) was observed followed by a slower reaction rate (k_2). Given the affinity of the product, 4-aminophenol, to the surface of Au catalysts, the slow reaction rate was attributed to the loss of active sites bound with 4-aminophenol.⁴⁵ As summarized in Fig. 7e, the k_1 for Au-P1, Au-P2, Au-CA and Au-P3 is -0.04 ± 0.006 s^{-1} , -0.03 ± 0.001 s^{-1} , -0.0077 ± 0.0012 s^{-1} , and -0.0018 ± 0.0001 s^{-1} , respectively (Table 2). Remarkably, Au-P1 was ~ 22 times more active than Au-P3 and ~ 5.2 times more active than Au-CA. Since the grafting densities of all three polymers are similar, the difference of their catalytic activity lies in the nature of binding motifs.

To confirm the impact of binding motifs in polymer ligands, we further examined the activity of polymer-modified PdNPs (Fig. S17–S20†). Similar to Au catalysts, both Pd-P1 and Pd-P2 quantitatively reduce 4-nitrophenol within 14 min while Pd-P3 and PdNPs need 50 min and 31 min, respectively to achieve full conversion. In addition, the k_1 for Pd-P1, Pd-P2, Pd-CA and Pd-P3 is -0.014 ± 0.001 s^{-1} , -0.012 ± 0.001 s^{-1} , -0.0043 ± 0.0006 s^{-1} , and -0.001 s^{-1} , respectively (Table 2). The variation tendency of the reduction rate for the Pd catalyst was similar to that of Au catalysts. The reduction rate of Pd-P1 was ~ 14 times that of Pd-P3 and ~ 3.3 times that of PdNPs, which further confirmed the positive effect of the Pd–NHC binding motif.

Due to the formation of Au–NHC bonds, both P1 and P2 modified catalysts exhibited optimal reaction rates compared to other control catalysts. It is well known that NHCs can bind the NPs through a metal–carbon bond and enrich the surface charge density of NPs by σ -donation.^{30,46–50} The enhanced performance of 4-nitrophenol reduction using NHC modified NPs can be explained by the increased electron density of the metal surface, resulting from charge transfer from the NHC ligand to the surface.^{14,26,51–54} Here, metal NPs such as AuNPs and PdNPs become stronger electron reservoirs, accelerating electron transfer from the donor (BH_4^-) to the acceptor (4-nitrophenol). The surface reaction of metal NPs between BH_4^- and H_2O generates BO_2^- and surface H-species.^{55–57} As pointed out by the previous reports,^{58,59} the enriched negative charges facilitate electron transport and enhance the affinity between metal–H species, which significantly improve the catalytic activity in 4-nitrophenol reduction.

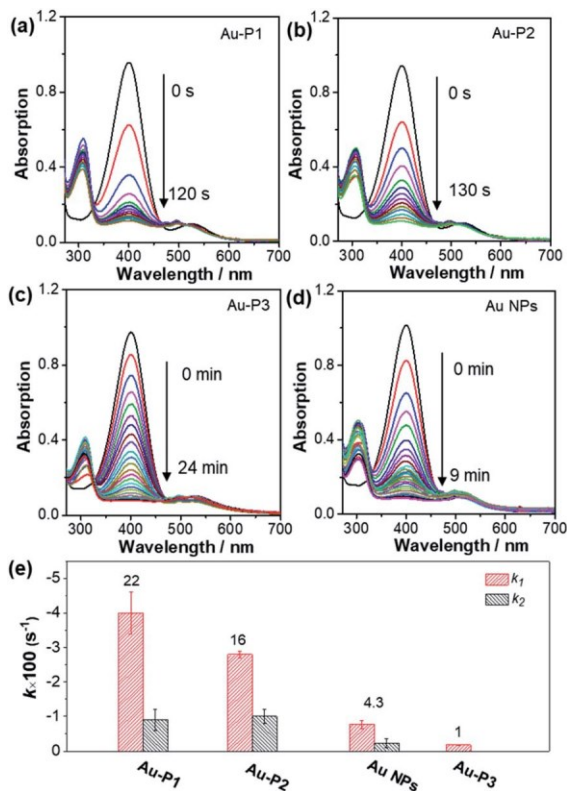


Fig. 7 UV-vis spectra of the reduction of 4-nitrophenol by using (a) Au-P1, (b) Au-P2, (c) Au-P3 and (d) AuNPs as catalysts, respectively. (e) Dependence of k versus the Au NPs modified with different ligands.

Conclusions

In summary, we have developed ligand exchange methods of colloidal noble metal NPs using polymeric NHCs and further demonstrated the uniqueness of polymeric NHC ligands in providing oxidative stability and promoting catalytic activity. Three PS ligands terminated with imidazolium bicarbonates, Cu–NHC groups and thiols were prepared through end-group functionalization. We found that the ligand exchange of PS–NHCs in poor solvents of polymers or at the biphasic interface is much faster compared to that of thiol-terminated PS. Remarkably, imidazolium-terminated PS can modify AuNPs within 2 min while 6 h is required to reach a similar grafting density to PS–SH. Our ligand exchange methods are highly versatile regardless of the compositions and sizes of noble metal NPs. Compared to the metal–thiolate binding, polymer NHC binding was demonstrated to be extremely stable under high temperature or oxidative conditions. Interestingly, all polymer ligands significantly crowded the surface of metal NPs; however, only polymer–NHC modified metal NPs showed improved activity. In the case of AuNPs, AuNPs modified with polymer NHCs are approximately 5.2 times more active than CA-capped ones and 22 times more active than those modified with Au–thiolate. In designing the ligand chemistry to control the catalytic properties of metal NPs, our results show the importance of binding motifs, particularly for polymer ligands, that has been overlooked in the past.

Experimental section

Synthesis of polymers and NPs

See ESI† for details.

Ligand modification with P1

A typical procedure to modify NPs with P1 is as follows. For CA capped AuNPs, 1 mL of P1 in THF (10 mg mL⁻¹) was quickly injected into 20 mL of 14 nm AuNP solution (0.1 mg mL⁻¹). The red precipitate of Au–P1 was collected after stirring for 2 min and purified by washing with THF four times. Finally, the Au–P1 with a concentration of 0.2 mg mL⁻¹ was obtained by re-dispersion in 10 mL of DMF. Note that the resulting Au–P1 can be easily transferred to other good solvents of PS by re-dispersion. Similarly, the modification of other NPs (e.g., different sizes of CA capped AuNPs, PdNPs and PtNPs) was carried out by changing the amount of P1 according to the concentration of NPs. The mass ratio of P1 and NPs was the same as that of 14 nm AuNPs.

To modify OAm capped AuNPs, a 4 mL hexane solution of AuNPs (0.3 mg mL⁻¹) was concentrated to about 0.2 mL through centrifugation and re-dispersed in 1 mL DCM. Subsequently, a 10 mL solution of P1 in DCM (1 mg mL⁻¹) was added dropwise into the above solution. After incubation overnight, Au–P1 was collected through centrifugation after washing with DMF 4 times.

Ligand modification with P2

A typical procedure to modify NPs with P2 is as follows. 10 mL of P2 in toluene (1 mg mL⁻¹) was poured into 20 mL of 14 nm AuNP solution (0.1 mg mL⁻¹). After stirring for 5 min, the toluene layer of Au–P2 was collected and purified by centrifugation with toluene four times. Finally, Au–P2 with a concentration of 0.2 mg mL⁻¹ was obtained by re-dispersion in 10 mL of DMF. Note that Au–P2 can be easily transferred to other good solvents of PS by centrifugation and re-dispersion. Similarly, the modification of other NPs was carried out by changing the amount of P2 according to the concentration of NPs. The mass ratio of P2 and NPs was the same as that of 14 nm AuNPs.

For the modification of OAm capped AuNPs, a 4 mL solution of AuNPs in hexane (0.3 mg mL⁻¹) was added into 3 mL DMF containing 10 mg of P2. After stirring for 30 min, the AuNPs transferred from the hexane layer (up) to the DMF layer (down). The Au–P2 was collected by centrifuging the DMF layer and washing with DMF 4 times.

Ligand modification with P3

A 20 mL aqueous solution of AuNPs (0.1 mg mL⁻¹) was concentrated to 0.3 mL through centrifugation and then added dropwise into a 10 mL solution of P3 in DMF (1 mg mL⁻¹). The solution was incubated for 2 h. After washing with DMF four times, the Au–P3 was re-dispersed in 10 mL of DMF with a concentration of 0.2 mg mL⁻¹ for further use.

Reduction of 4-nitrophenol

The catalytic activity of the NPs was evaluated through the reduction of 4-nitrophenol to 4-aminophenol by NaBH₄ as a model reaction. Typically, 1 mL of 0.1 mM 4-nitrophenol solution was first added into a quartz cuvette. Then, 1 mL of 30 mM NaBH₄ was injected into the above solution, whose color was changed from light yellow to dark yellow due to the formation of the 4-nitrophenolate ion. The reaction kinetics was monitored by in situ UV-vis spectroscopy at a fixed interval after adding 50 mL of Au catalysts (0.2 mg mL⁻¹) or Pd catalysts (0.03 mg mL⁻¹).

Characterization

TEM was carried out on a FEI Tecnai 12 G2 Spirit BioTWIN. Proton and carbon NMR spectra were recorded on a Bruker Avance 400 MHz spectrometer. HMBC spectra were collected using a Varian INOVA 600 MHz spectrometer. All NMR experiments were carried out in CDCl₃. UV-vis spectroscopy was conducted with a Cary 60 UV-Vis spectrophotometer. TGA was performed to heat the samples from 100 °C to 700 °C at a heating rate of 10 °C under N₂ using a TA Instrument TGA Q-500. Before collection of TGA, the sample was annealed at 100 °C for 1 h to remove residual solvents. SEC measurements were carried out on a Waters SEC-1 (1515 HPLC pump and Waters 717Plus auto injector) equipped with a Varian 380-LC evaporative light scattering detector and three Jordi Gel μuorinated DVB columns (1–100k, 2–10k, and 1–500 Å). THF was employed as an elution solvent under a flow rate of 1.25

mL min⁻¹, and the data were processed using Empower SEC software (Waters, Inc.).

Conflicts of interest

There are no conflicts to declare.

Acknowledgements

JH is grateful for the financial support from the ACS Petroleum Research Fund (ACS PRF) and US National Science Foundation (CBET-1705566 and 1936228). The TEM studies were carried out at the Biosciences Electron Microscopy Facility at the University of Connecticut.

References

- C. Rogers, W. S. Perkins, G. Veber, T. E. Williams, R. R. Cloke and F. R. Fischer, *J. Am. Chem. Soc.*, 2017, **139**, 4052–4061.
- J. A. Trindell, J. Clausmeyer and R. M. Crooks, *J. Am. Chem. Soc.*, 2017, **139**, 16161–16167.
- L. Jin, B. Liu, S. Duay and J. He, *Catalysts*, 2017, **7**, 44.
- Z. Niu and Y. Li, *Chem. Mater.*, 2013, **26**, 72–83.
- J. A. Lopez-Sanchez, N. Dimitratos, C. Hammond, G. L. Brett, L. Kesavan, S. White, P. Miedziak, R. Tiruvalam, R. L. Jenkins, A. F. Carley, D. Knight, C. J. Kiely and G. J. Hutchings, *Nat. Chem.*, 2011, **3**, 551–556.
- K. R. Kahsar, D. K. Schwartz and J. W. Medlin, *ACS Catal.*, 2013, **3**, 2041–2044.
- D. Li, C. Wang, D. Tripkovic, S. Sun, N. M. Markovic and V. R. Stamenkovic, *ACS Catal.*, 2012, **2**, 1358–1362.
- B. Liu, H. Yao, W. Song, L. Jin, I. M. Mosa, J. F. Rusling, S. L. Suib and J. He, *J. Am. Chem. Soc.*, 2016, **138**, 4718–4721.
- T. Yoskamtorn, S. Yamazoe, R. Takahata, J.-i. Nishigaki, A. Thivasasith, J. Limtrakul and T. Tsukuda, *ACS Catal.*, 2014, **4**, 3696–3700.
- S. M. Ansar and C. L. Kitchens, *ACS Catal.*, 2016, **6**, 5553–5560.
- X. Pang, L. Zhao, W. Han, X. Xin and Z. Lin, *Nat. Nanotechnol.*, 2013, **8**, 426–431.
- M. Wang, X. Pang, D. Zheng, Y. He, L. Sun, C. Lin and Z. Lin, *J. Mater. Chem. A*, 2016, **4**, 7190–7199.
- L. Liu, Z. Gao, B. Jiang, Y. Bai, W. Wang and Y. Yin, *Nano Lett.*, 2018, **18**, 5312–5318.
- C. Yi, Y. Yang, B. Liu, J. He and Z. Nie, *Chem. Soc. Rev.*, 2020, **49**, 465–508.
- L. Zhang, Z. Wei, S. Thanneeru, M. Meng, M. Kruzyk, G. Ung, B. Liu and J. He, *Angew. Chem., Int. Ed. Engl.*, 2019, **131**, 15981–15987.
- S. Wu, J. Dzubiella, J. Kaiser, M. Drechsler, X. Guo, M. Ballauff and Y. Lu, *Angew. Chem., Int. Ed. Engl.*, 2012, **51**, 2229–2233.
- A. R. Riscoe, C. J. Wrasman, A. A. Herzog, A. S. Hoffman, A. Menon, A. Boubnov, M. Vargas, S. R. Bare and M. Cargnello, *Nat. Catal.*, 2019, **2**, 852–863.
- Z. Nie, D. Fava, E. Kumacheva, S. Zou, G. C. Walker and M. Rubinstein, *Nat. Mater.*, 2007, **6**, 609–614.
- R. M. Choueiri, E. Galati, H. Therien-Aubin, A. Klinkova, E. M. Larin, A. Querejeta-Fernandez, L. Han, H. L. Xin, O. Gang, E. B. Zhulina, M. Rubinstein and E. Kumacheva, *Nature*, 2016, **538**, 79–83.
- J.-S. Lee, A. K. R. Lytton-Jean, S. J. Hurst and C. A. Mirkin, *Nano Lett.*, 2007, **7**, 2112–2115.
- A. Kassam, G. Bremner, B. Clark, G. Ulibarri and R. B. Lennox, *J. Am. Chem. Soc.*, 2006, **128**, 3476–3477.
- J. Song, J. Zhou and H. Duan, *J. Am. Chem. Soc.*, 2012, **134**, 13458–13469.
- Z. Wang, B. He, G. Xu, G. Wang, J. Wang, Y. Feng, D. Su, B. Chen, H. Li, Z. Wu, H. Zhang, L. Shao and H. Chen, *Nat. Commun.*, 2018, **9**, 563.
- B. Liu, S. Thanneeru, A. Lopes, L. Jin, M. McCabe and J. He, *Small*, 2017, **13**, 1700091.
- H. Hakkinen, *Nat. Chem.*, 2012, **4**, 443–455.
- S. Engel, E. C. Fritz and B. J. Ravoo, *Chem. Soc. Rev.*, 2017, **46**, 2057–2075.
- D. J. Lavrich, S. M. Wetterer, S. L. Bernasek and G. Scoles, *J. Phys. Chem. B*, 1998, **102**, 3456–3465.
- C. M. Crudden, J. H. Horton, M. R. Narouz, Z. Li, C. A. Smith, K. Munro, C. J. Baddeley, C. R. Larrea, B. Drevniok, B. Thanabalasingam, A. B. McLean, O. V. Zenkina, I. I. Ebralidze, Z. She, H.-B. Kraatz, N. J. Mosey, L. N. Saunders and A. Yagi, *Nat. Commun.*, 2016, **7**, 12654.
- M. N. Hopkinson, C. Richter, M. Schedler and F. Glorius, *Nature*, 2014, **510**, 485–496.
- C. A. Smith, M. R. Narouz, P. A. Lummis, I. Singh, A. Nazemi, C. H. Li and C. M. Crudden, *Chem. Rev.*, 2019, **119**, 4986–5056.
- J. He, Y. Liu, T. Babu, Z. Wei and Z. Nie, *J. Am. Chem. Soc.*, 2012, **134**, 11342–11345.
- S. Thanneeru, K. M. Ayers, M. Anuganti, L. Zhang, C. V. Kumar, G. Ung and J. He, *J. Mater. Chem. C*, 2020, **8**, 2280–2288.
- A. Bakker, A. Timmer, E. Kolodzeiski, M. Freitag, H. Y. Gao, H. Mönig, S. Amirjalayer, F. Glorius and H. Fuchs, *J. Am. Chem. Soc.*, 2018, **140**, 11889–11892.
- Z. Huang, D. Raciti, S. Yu, L. Zhang, L. Deng, J. He, Y. Liu, N. M. Khashab, C. Wang, J. Gong and Z. Nie, *J. Am. Chem. Soc.*, 2016, **138**, 6332–6335.
- J. He, X. Huang, Y.-C. Li, Y. Liu, T. Babu, M. A. Aronova, S. Wang, Z. Lu, X. Chen and Z. Nie, *J. Am. Chem. Soc.*, 2013, **135**, 7974–7984.
- S. Minko, in *Polymer Surfaces and Interfaces: Characterization, Modification and Applications*, ed. M. Stamm, Springer Berlin Heidelberg, Berlin, Heidelberg, 2008, pp. 215–234, DOI: 10.1007/978-3-540-73865-7_11.
- G. Frens, *Nature, Phys. Sci.*, 1973, **241**, 20–22.
- J. Turkevich and G. Kim, *Science*, 1970, **169**, 873–879.
- G. W. Wu, S. B. He, H. P. Peng, H. H. Deng, A. L. Liu, X. H. Lin, X. H. Xia and W. Chen, *Anal. Chem.*, 2014, **86**, 10955–10960.
- M. Borzenkov, G. Chirico, L. D'Alfonso, L. Sironi, M. Collini, E. Cabrini, G. Dacarro, C. Milanese, P. Pallavicini, A. Taglietti, C. Bernhard and F. Denat, *Langmuir*, 2015, **31**, 8081–8091.

- 41 Y. Que, C. Feng, S. Zhang and X. Huang, *J. Phys. Chem. C*, 2015, **119**, 1960–1970.
- 42 Y. Chen, Z. Wang, Y. W. Harn, S. Pan, Z. Li, S. Lin, J. Peng, G. Zhang and Z. Lin, *Angew. Chem., Int. Ed. Engl.*, 2019, **58**, 11910–11917.
- 43 S. Wunder, Y. Lu, M. Albrecht and M. Ballauff, *ACS Catal.*, 2011, **1**, 908–916.
- 44 S. Wunder, F. Polzer, Y. Lu, Y. Mei and M. Ballauff, *J. Phys. Chem. C*, 2010, **114**, 8814–8820.
- 45 P. Suchomel, L. Kvitek, R. Pucek, A. Panacek, A. Halder, S. Vajda and R. Zboril, *Sci. Rep.*, 2018, **8**, 4589.
- 46 A. Ferry, K. Schaepe, P. Tegeder, C. Richter, K. M. Chopiga, B. J. Ravoo and F. Glorius, *ACS Catal.*, 2015, **5**, 5414–5420.
- 47 J. B. Ernst, S. Muratsugu, F. Wang, M. Tada and F. Glorius, *J. Am. Chem. Soc.*, 2016, **138**, 10718–10721.
- 48 Z. Cao, D. Kim, D. Hong, Y. Yu, J. Xu, S. Lin, X. Wen, E. M. Nichols, K. Jeong, J. A. Reimer, P. Yang and C. J. Chang, *J. Am. Chem. Soc.*, 2016, **138**, 8120–8125.
- 49 Z. Cao, J. S. Derrick, J. Xu, R. Gao, M. Gong, E. M. Nichols, P. T. Smith, X. Liu, X. Wen and C. Copéret, *Angew. Chem., Int. Ed. Engl.*, 2018, **57**, 4981–4985.
- 50 A. Rühling, K. Schaepe, L. Rakers, B. Vonhören, P. Tegeder, B. J. Ravoo and F. Glorius, *Angew. Chem., Int. Ed. Engl.*, 2016, **55**, 5856–5860.
- 51 S. G. Song, C. Satheeshkumar, J. Park, J. Ahn, T. Premkumar, Y. Lee and C. Song, *Macromolecules*, 2014, **47**, 6566–6571.
- 52 Z. Cao, J. S. Derrick, J. Xu, R. Gao, M. Gong, E. M. Nichols, P. T. Smith, X. Liu, X. Wen, C. Copéret and C. J. Chang, *Angew. Chem., Int. Ed. Engl.*, 2018, **57**, 4981–4985.
- 53 A. V. Zhukhovitskiy, M. J. MacLeod and J. A. Johnson, *Chem. Rev.*, 2015, **115**, 11503–11532.
- 54 R. Zhong, A. C. Lindhorst, F. J. Groche and F. E. Kuhn, *Chem. Rev.*, 2017, **117**, 1970–2058.
- 55 M. Kohantorabi and M. R. Gholami, *New J. Chem.*, 2017, **41**, 10948–10958.
- 56 T. A. Revathy, T. Sivaranjani, A. A. Boopathi, S. Sampath, V. Narayanan and A. Stephen, *RSC Adv.*, 2018, **45**, 815–832.
- 57 S. Vivek, P. Arunkumar and K. S. Babu, *RSC Adv.*, 2016, **6**, 45947–45956.
- 58 X.-k. Kong, Z.-y. Sun, M. Chen, C.-l. Chen and Q.-w. Chen, *Energy Environ. Sci.*, 2013, **6**, 3260.
- 59 R. Ciganda, N. Li, C. Deraedt, S. Gatard, P. Zhao, L. Salmon, R. Hernandez, J. Ruiz and D. Astruc, *Chem. Commun.*, 2014, **50**, 10126–10129.